Toxicology Letters 286 (2018) 39–47

Contents lists available at ScienceDirect

Toxicology Letters

journal homepage: www.elsevier.com/locate/toxlet

# Intravascular hemolysis induced by phospholipases $A_2$ from the venom of the Eastern coral snake, *Micrurus fulvius*: Functional profiles of hemolytic and non-hemolytic isoforms

María Laura Fernández[a], Pablo Yunes Quartino[b], Ruth Arce-Bejarano[a], Julián Fernández[a], Luis F. Camacho[a], José María Gutiérrez[a], Daniel Kuemmel[c], Gerardo Fidelio[b], Bruno Lomonte[a,*]

[a] *Instituto Clodomiro Picado, Facultad de Microbiología, Universidad de Costa Rica San José 11501, Costa Rica*
[b] *Centro de Investigaciones en Química Biológica de Córdoba (CIQUIBIC), Departamento de Química Biológica, Facultad de Ciencias Químicas, Universidad Nacional de Córdoba, Argentina*
[c] *Biology and Chemistry Department, University of Osnabrueck, Osnabrueck, Germany*

## GRAPHICAL ABSTRACT


## ARTICLE INFO

*Keywords:*
Venom
Coral snake
*Micrurus fulvius*
Phospholipase $A_2$
Intravascular hemolysis
Toxicity
Membrane damage

## ABSTRACT

A unique feature of the venom of *Micrurus fulvius* (Eastern coral snake) is its ability to induce severe intravascular hemolysis in particular species, such as dogs or mice. This effect was previously shown to be induced by distinct phospholipase $A_2$ ($PLA_2$) isoforms which cause direct hemolysis *in vitro*, an uncommon finding for such enzymes. The functional profiles of $PLA_2$-17, a direct hemolytic enzyme, and $PLA_2$-12, a co-existing venom isoform lacking such effect, were compared. The enzymes differed not only in their ability to cause intravascular hemolysis: $PLA_2$-17 additionally displayed lethal, myotoxic, and anticoagulant actions, whereas $PLA_2$-12 lacked these effects. $PLA_2$-12 was much more active in hydrolyzing a monodisperse synthetic substrate than $PLA_2$-17, but the catalytic activity of latter was notably higher on a micellar substrate, or towards pure phospholipid artificial monolayers under controlled lateral pressures. Interestingly, $PLA_2$-17 could hydrolyze substrate at a pressure of 20 mN $m^{-1}$, in contrast to $PLA_2$-12 or the non-toxic pancreatic $PLA_2$. This suggests important differences in the monolayer penetrating power, which could be related to differences in toxicity. Comparative examination of primary structures and predicted three-dimensional folding of $PLA_2$-12 and $PLA_2$-17, revealed that differences concentrate in their N-terminal and central regions, leading to variations of the surface properties at the membrane interacting interface. $PLA_2$-17 presents a less basic interfacial surface than $PLA_2$-12, but more bulky aromatic residues, which could be associated to its higher membrane-penetrating strength. Altogether, these structural and functional comparative observations suggest that the ability of $PLA_2$s to penetrate substrate interfaces could be a major determinant of toxicity, perhaps more important than protein surface charge.

* Corresponding author.
*E-mail address:* bruno.lomonte@ucr.ac.cr (B. Lomonte).

https://doi.org/10.1016/j.toxlet.2017.11.037
Received 4 September 2017; Received in revised form 10 November 2017; Accepted 27 November 2017
Available online 29 November 2017
0378-4274/ 

## 1. Introduction

Phospholipases $A_2$ ($PLA_2$; EC 3.1.1.4) are present in the vast majority of snake venoms, displaying a wide spectrum of toxic activities of clinical relevance such as neurotoxicity, myotoxicity, proinflammatory effects, and hemostasis alterations, among others (Kini, 2003; Montecucco et al., 2008). In spite of the large number of snake venom $PLA_2$s isolated and biochemically characterized, current understanding on the mechanisms underlying their diverse and specific toxic effects is still limited (Gutiérrez and Lomonte, 2013). Largely unknown, the identification of their key structural motifs responsible for distinct toxic effects, and their relevant molecular targets, represents a current challenge in toxinological research.

An uncommon, although medically relevant toxic effect reported for some snake venom $PLA_2$s is intravascular hemolysis. Only a few (Condrea et al., 1981; Gao et al., 1999; Arce-Bejarano et al., 2014) of the more than 350 snake venom $PLA_2$s currently listed in the UniProt databases (http://www.uniprot.org/) have been shown to induce this effect *in vivo*. In all cases, these directly hemolytic enzymes belong to the structural group I of secreted $PLA_2$s, which are found in the venoms from snakes of the Elapidae family (Kini, 2003), sharing structural homology with the secreted pancreatic $PLA_2$s of mammals (Križaj, 2014).

In a previous study, the intravascular hemolysis induced by the venom of the North American 'Eastern coral snake' (*Micrurus fulvius*) in a mouse model was investigated. Hemolysis was adscribed to the presence of particular $PLA_2$ isoforms, one of which was isolated and sequenced (Arce-Bejarano et al., 2014). The purified enzyme reproduced the strong hemolytic effect induced by the whole venom upon intravenous injection in mice. Dog erythrocytes were shown to be also highly susceptible to the lytic action of the venom, in agreement with veterinary clinical reports on envenomings by *M. fulvius* in this species (Marks et al., 1990; Peterson, 2006; Pérez et al., 2012). However, *M. fulvius* venom did not induce hemolysis in rabbit, horse, or human erythrocytes, revealing important differences in the species susceptibility to the hemolytic effect (Arce-Bejarano et al., 2014). Intriguingly, to date no other venom from coral snake (*Micrurus*) species has been reported to induce intravascular hemolysis *in vivo* (Lomonte et al., 2016). Therefore, the directly hemolytic $PLA_2$s found in *M. fulvius* venom provide a unique opportunity for investigating the structural and functional characteristics that endow these enzymes with such uncommon toxic activity.

Phylogenetically, *M. fulvius* clusters within a group of coral snake species whose venoms are predominantly composed by $PLA_2$s, in contrast to species that produce venoms highly rich in three-finger toxins (Fernández et al., 2015; Lomonte et al., 2016). In fact, venom gland transcriptomic analyses revealed that *M. fulvius* may secrete a large diversity of $PLA_2$ isoforms, with more than 50 different transcript sequences reported (Margres et al., 2013). In previous chromatographic fractionation of this venom (Arce-Bejarano et al., 2014), at least three major $PLA_2$ protein peaks were found to display direct hemolytic activity in mice, of which one (peak 17) was fully sequenced and corresponds to '$PLA_2$-2b' (access code U3EPF0) of the transcriptomic database generated by Margres et al. (2013). Another major venom $PLA_2$ (peak 12) was found to be devoid of hemolytic activity. Considering their marked difference in the ability to induce intravascular hemolysis, the aim of the present study was to compare the functional profile and some structural features of these two $PLA_2$ isoforms present in *M. fulvius* venom, to gain further insights into the basis of this toxic activity.

## 2. Materials and methods

### 2.1. Venom

Two batches of lyophilized *M. fulvius* venoms were used along these studies: one was purchased from Sigma-Aldrich (Missouri, USA) and the other was donated by the Division of Biological Standards, National Institutes of Health, USA. Both venoms were stored at −20 °C and dissolved immediately before use. In order to ascertain their similarity, the two venom batches were comparatively analyzed by SDS-PAGE on a gradient (8–16%) gel (Laemmli, 1970), under non-reducing or reducing conditions, using Coomassie blue G-250 for protein staining.

### 2.2. Isolation of phospholipases $A_2$

*M. fulvius* venom was fractionated by RP-HPLC as described previously (Arce-Bejarano et al., 2014). Briefly, 2 mg of venom was dissolved in 200 µL of water containing 0.1% trifluoroacetic acid (TFA) (solvent A), and separated in a $C_{18}$ column (4.6 × 250 mm, 5 µm particle; Phenomenex) using an Agilent 1200 chromatograph and monitoring at 215 nm. Elution was carried out at 1 mL/min by applying the following gradient toward acetonitrile with 0.1% TFA (solvent B): 0% B for 5 min, 0–15% B over 10 min, 15–45% B over 60 min, 45–70% B over 10 min, and 70% B over 9 min. Fractions (peaks 12 and 17, as numbered in Arce-Bejarano et al., 2014) were collected manually, dried by vacuum centrifugation at 45 °C, and redissolved in 0.12 M NaCl, 0.04 M sodium phosphate (PBS, pH 7.2) for further characterization. Protein concentration of the enzymes was adjusted by measuring their absorbance at 280 nm on a NanoDrop 2000c reader (Thermo Scientific).

### 2.3. Identification of $PLA_2$-12 by tandem mass spectrometry

The hemolytic $PLA_2$ from peak 17 was previously identified as '$PLA_2$-2b' (access code U3EPF0) by matching its complete amino acid sequence (Arce-Bejarano et al., 2014) with data from the venom gland transcriptome of *M. fulvius* (Margres et al., 2013). A similar approach was undertaken for the non-hemolytic $PLA_2$ from peak 12. The protein was dissolved in ammonium bicarbonate (50 mM), reduced with dithiothreitol (10 mM) at 60 °C for 20 min, and alkylated with iodoacetamide (50 mM) in the dark for 20 min (Van der Laat et al., 2013). Then, it was subjected to digestion with sequencing grade trypsin (Sigma) overnight at 37 °C, or chymotrypsin (G-Biosciences) for 2 h at 30 °C. Resulting peptides were separated by RP-HPLC on a $C_{18}$ column (2.1 × 150 mm) and finally analyzed by MALDI-TOF/TOF mass spectrometry on an Applied Biosystems 4800 Plus Proteomics Analyzer, in positive reflector mode, as described (Arce-Bejarano et al., 2014).

### 2.4. Animal experiments

Animal experiments were conducted using CD-1 mice of either sex (16–18 g), following protocols approved by the Institutional Committee for the Use and Care of Animals (CICUA, 152-2015), University of Costa Rica. Mice were housed in groups of four or five, and provided food and water *ad libitum*. After experiments, mice were euthanized by $CO_2$ inhalation.

### 2.5. Intravascular hemolytic activity

The enzymes $PLA_2$-12 or $PLA_2$-17 (5 µg), respectively, were injected by the intravenous (i.v.) route, in 100 µL of PBS, in groups of four mice. A control group received an identical injection of 100 µL of PBS alone. After one h, mice were bled from the tip of the tail into heparinized capillary tubes, which were centrifuged to determine hematocrit values. In the case of $PLA_2$-17, the time-course for recovery of the acute hematocrit drop was monitored by injecting 2.5 µg i.v. (a sublethal dose) in a group of four mice, in 100 µL of PBS, followed by measurements performed at 1, 24, 48, 72 h, and one week later.

### 2.6. Lethal activity

The lethal potency of $PLA_2$-12 or $PLA_2$-17 was tested by i.v. injection of various doses (2.5–25 µg), dissolved in 100 µL of PBS, in groups

of four mice. A control group received an identical injection of PBS alone. Deaths were recorded after 48 h, and the median lethal dose ($LD_{50}$) was estimated by probit analysis, using Biostat v.5.2 (AnalystSoft).

### 2.7. Myotoxic activity

The enzymes $PLA_2$-12 or $PLA_2$-17 (10 μg), respectively, were injected into the gastrocnemius muscle of groups of five mice, in 50 μL of PBS. A control group received an identical injection of PBS alone. After three h, blood samples were obtained from the tip of the tail into heparinized capillary tubes and centrifuged. The plasma creatine kinase (CK) activity, expressed in U/L, was determined using a UV kinetic assay (CKNac, Biocon Diagnostik) as described (Gutiérrez et al., 1986).

### 2.8. Anticoagulant activity on plasma

The anticoagulant activity of $PLA_2$-12 or $PLA_2$-17 was assayed on citrated platelet-poor human plasma (PPHP), obtained from healthy donors. Varying amounts of the corresponding enzyme (0.065–2 μg), dissolved in 20 μL of water, were added to 200 μL of PPHP, and incubated at 37 °C for 10 min. Then, 40 μL of 250 mM $CaCl_2$ was added and coagulation times were recorded, in triplicate assays, as described (Gutiérrez et al., 1986).

### 2.9. Bactericidal activity

The bactericidal activity of $PLA_2$-12 and $PLA_2$-17 against *Escherichia coli* (Gram-negative) and *Staphylococcus aureus* (Gram-positive) was assayed by an agar diffusion test (Vargas et al., 2012). Each isolated enzyme (10 μg), dissolved in 10 μL of sterile PBS, was added as a droplet onto Luria-Bertani agar plates previously streaked with the corresponding bacterial suspensions. The crude venom of *M. fulvius* (50 μg), dissolved in 10 μL of sterile PBS, was used as a positive control, whereas sterile PBS alone was used as a negative control. Growth inhibition halos were recorded after 24 h of incubation at 37 °C.

### 2.10. Phospholipase $A_2$ activity on NOBA

The enzymatic activity of $PLA_2$-12 and $PLA_2$-17 was determined on the monodisperse synthetic substrate 4-nitro-3-octanoyloxy-benzoic acid (NOBA), as previously described (Mora-Obando et al., 2014). Varying amounts of the corresponding enzyme (1–8 μg), dissolved in 25 μL of water, were added to 200 μL of reaction buffer (10 mM Tris, 10 mM $CaCl_2$, 0.1 M NaCl, pH 8.0), in triplicate wells of a microplate. After mixing, 25 μL of NOBA (1 mg/mL in acetonitrile) were added, to achieve a final substrate concentration of 0.32 mM. Substrate incubated with 25 μL of water was used as a control. The mixtures were incubated for 60 min at 37 °C, and absorbances at 405 nm were recorded. $PLA_2$ activity was expressed as the final change in absorbance.

### 2.11. Phospholipase $A_2$ activity on phosphatidylcholine micelles

The enzymatic activity of $PLA_2$-12 and $PLA_2$-17 was determined on micellar phosphatidylcholine, as previously described (Rey-Suárez et al., 2016). Varying amounts of the corresponding enzyme (0.25–4 μg), dissolved in 20 μL of water, were added to 1 mL of substrate (0.25% w/v *sn*-3-phosphatidylcholine, 0.4% v/v Triton X-100, 0.004% w/v phenol red) in a thermoregulated cuvette at 30 °C. Substrate incubated with 20 μL of water was used as a control. The absolute value of the change in absorbance at 558 nm was determined after 1 min, in triplicate assays.

### 2.12. Phospholipid hydrolysis in dilauroyl-phosphatidylcholine monolayers

Hydrolysis of dilauroyl phosphatidylcholine (DLPC) monolayers by $PLA_2$-12 or $PLA_2$-17 was evaluated at lipid constant lateral pressure (barostatic mode) essentially as described by Yunes Quartino et al. (2015). Data collection and barrier control was performed with a KSV layer builder apparatus (Biolin Scientifc Ab). Briefly, DLPC (850335P, Avanti Polar Lipids) was dissolved at 0.1 mM in chloroform, and carefully spread with a Hamilton syringe onto the surface of an aqueous solution of 100 mM NaCl, 20 mM $CaCl_2$, 10 mM Tris, pH 8.0 (at 25 °C), in a Teflon trough with a rectangular reservoir (31.2 $cm^2$) connected to a smaller circular reaction reservoir (3.8 $cm^2$) by a narrow and shallow channel (0.5 $cm^2$). Lateral compression of the surface DLPC film was achieved by a single Teflon movable barrier, electronically controlled. After lipid spreading, the lateral pressure was set up either to 10 mN $m^{-1}$ or 20 mN $m^{-1}$, and maintained constant through the course of the experiment. After 10 min (baseline drift), 10 μL of a 0.3 μg/μL solution of the corresponding enzyme, in 50 mM ammonium formate, pH 4.5, was injected below the surface of the reaction compartment, under constant magnetic stirring. This was defined as time = 0. The change in area (due to movement of the barrier compensating lateral pressure) was recorded, indicating DLPC hydrolysis.

Surface density (Ns) in molecules $cm^{-2}$ is related to lateral pressure (Π) in mN $m^{-1}$ in our case by the following equation: $Ns = 1 \times 1014 \times (3.84–2.8 \times e(-\Pi)/112.5)-1.04 \times e(-\Pi)/0.11$. The hydrolysis rate was the slope ($cm^2\ s^{-1}$) of the linear portion of the area *vs*. time curve after enzyme injection corrected by the slope prior enzyme. This rate was converted into molecules $s^{-1}$ by multiplying it by the DLPC surface density according to the previous equation. Lag time was calculated as the time of intercept of the fitted line prior enzyme injection and the line after injection that shows a linear portion using a minimum of 180 points (3 min measurement as a minimum), checking the residual to be $R \geq 0.997$.

### 2.13. Homology modeling of $PLA_2$-12 and $PLA_2$-17

Models of $PLA_2$-12 and $PLA_2$-17 from *M. fulvius* were generated using SWISS-MODEL (Arnold et al., 2006). The ligand in the substrate binding site was modeled based on a superposition with the structure of a $PLA_2$ from *N. atra* in complex with the transition state analogue L-1-*O*-octyl-2-heptylphosphonyl-sn-*glycero*-3-phosphoethanolamine (PDBID 1POB; White et al., 1990). Electrostatic surface potential maps were calculated with APBS (Baker et al., 2001). All figures of molecular models were generated using PyMOL (DeLano, 2003).

### 2.14. Statistical analyses

The statistical significance of differences recorded between more than two experimental groups was determined by ANOVA, followed by Tukey *post-hoc* tests, at a level of $p < 0.05$, using the software InStat v.3.05 (GraphPad).

## 3. Results

### 3.1. Isolation and identification of $PLA_2$s

Following the chromatographic conditions described by Arce-Bejarano et al. (2014), $PLA_2$s from peaks 12 and 17 were isolated and comparatively characterized. The two venom batches used as starting material did not show significant variations when compared by SDS-PAGE (Supplementary Fig. S1), also resulting in consistent chromatographic patterns in RP-HPLC fractionation. $PLA_2$-17 was previously shown to correspond to '$PLA_2$-2b' (U3EPF0) of the venom gland transcriptome of *M. fulvius* (Margres et al., 2013). On the other hand, the partial amino acid sequence obtained for $PLA_2$-12 after digestion with trypsin and chymotrypsin, followed by MALDI-TOF/TOF analysis (Supplementary Fig. S2), matched a single sequence of the transcriptome, therefore supporting its identity with '$PLA_2$-24' (U3FYP5). To facilitate their identification according to the protein elution profile

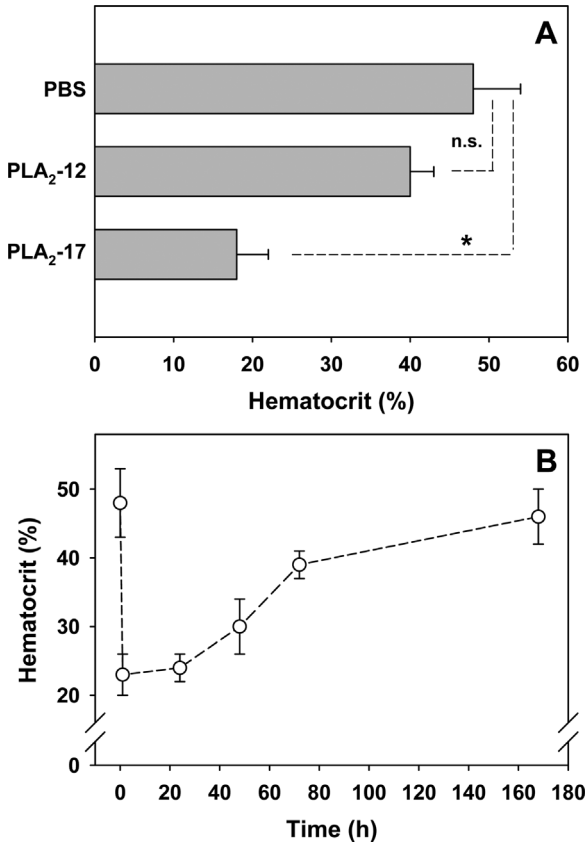


**Fig. 1.** Evaluation of intravascular hemolysis after the i.v. injection of $PLA_2$-12 or $PLA_2$-17 in mice. **(A)** Hematocrit values determined 1 h after the injection of 5 μg of each enzyme, or PBS alone. Each bar represents the mean ± SD of four animals. The difference between hematocrit values of mice that received $PLA_2$-12 or PBS is not statistically significant (n.s.; $p > 0.05$ by Tukey *post-hoc* test after ANOVA), whereas the reduction of hematocrit caused by $PLA_2$-17 is highly significant (*; $p < 0.01$). **(B)** Evaluation of the recovery of hematocrit values in mice after the i.v. injection of 2.5 μg of $PLA_2$-17. Each point represents mean ± SD of four animals.

after RP-HPLC separation of the venom, the two *M. fulvius* enzymes will be herein referred to as $PLA_2$-12 and $PLA_2$-17, following the previous description of Arce-Bejarano et al. (2014).

### 3.2. Toxic activities

When tested for hemolytic activity *in vivo*, $PLA_2$-17 induced a severe drop in blood hematocrit after i.v. injection (Fig. 1a), confirming previous results (Arce-Bejarano et al., 2014). In contrast, i.v. injection of $PLA_2$-12 did not result in any significant alteration of the hematocrit (Fig. 1a) or coloration of plasma, indicating its lack of hemolytic activity. Intense colored reddish urine was observed in mice injected with 5 μg of $PLA_2$-17, but not in those injected with $PLA_2$-12, which showed urine of normal pale yellow coloration. The dramatic drop in hematocrit induced by a sublethal i.v. dose of $PLA_2$-17 (2.5 μg) gradually recovered to normal values by one week (Fig. 1b).

In addition to its intravascular hemolytic effect, $PLA_2$-17 showed high lethality in mice (Table 1), with an estimated i.v. $LD_{50}$ of 5 μg/mouse or 0.3 μg/g body weight. In contrast, no deaths or signs of toxicity were recorded in mice receiving i.v. injections of much higher doses of $PLA_2$-12, up to 25 μg/mouse (1.5 μg/g) (Table 1).

A further sharp difference between $PLA_2$-12 and $PLA_2$-17 was observed regarding myotoxic activity. The latter enzyme induced a high increment in the plasma creatine kinase (CK) activity of mice after intramuscular injection (Fig. 2). $PLA_2$-12, in contrast, induced a minor elevation of plasma CK, which did not reach statistical significance in comparison to control animals that received PBS alone (Fig. 2).

**Table 1**
Evaluation of lethal activity of $PLA_2$-12 and $PLA_2$-17 from *Micrurus fulvius* venom in mice,[a] injected by the i.v. route.

| | Dead/Injected Mice (48 h) | |
|---|---|---|
| Enzyme dose | $PLA_2$-12 | $PLA_2$-17 |
| 2.5 μg | n.t. | 0/4 |
| 5.0 μg | 0/4 | 2/4 |
| 12.5 μg | n.t. | 4/4 |
| 25.0 μg | 0/4 | 4/4 |

n.t.: not tested.
[a] 16–18 g body weight.

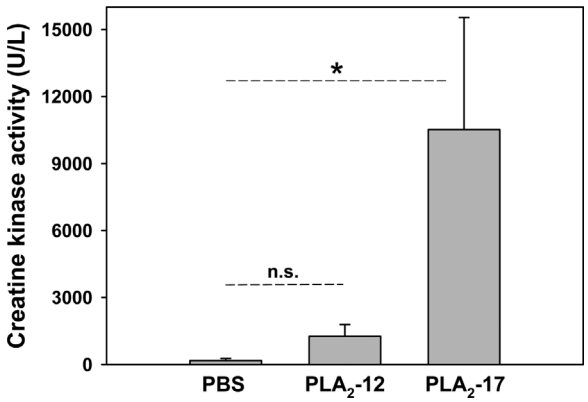


**Fig. 2.** Evaluation of myotoxicity after the i.m. injection of $PLA_2$-12 or $PLA_2$-17 in mice. Plasma creatine kinase (CK) activity was determined 3 h after the injection of 10 μg of each enzyme, or PBS alone. Each bar represents mean ± SD of five animals. The difference between CK values of mice that received $PLA_2$-12 or PBS is not statistically significant (n.s.; $p > 0.05$ by Tukey *post-hoc* test after ANOVA). The increase in CK values induced by $PLA_2$-17 is highly significant (*; $p < 0.01$) in comparison to the PBS control.

### 3.3. In vitro activities

$PLA_2$-17 displayed a potent anticoagulant effect when incubated with human platelet-poor plasma, affecting the recalcification time, whereas under identical conditions $PLA_2$-12 completely lacked this activity (Fig. 3).

The whole venom of *M. fulvius* displayed a bactericidal effect against both *E. coli* and *S. aureus*, producing growth inhibition halos. However, neither of the two $PLA_2$ enzymes had any visible effect on the bacteria after 24 h of growth (results not shown).

The enzymatic activity of $PLA_2$-12 and $PLA_2$-17 was comparatively

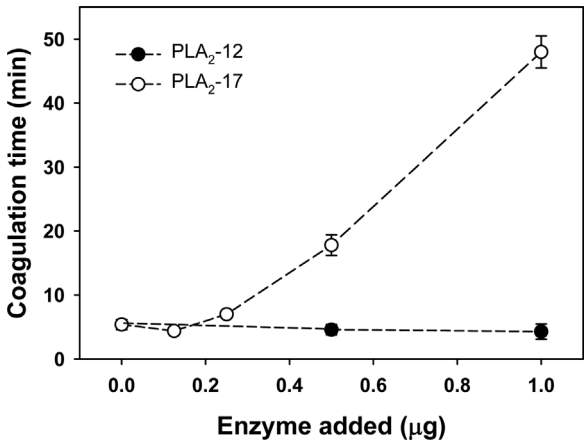


**Fig. 3.** Evaluation of anticoagulant activity of $PLA_2$-12 or $PLA_2$-17 in human platelet-poor plasma. Enzymes were incubated with the plasma for 10 min at 37 °C, and after the addition of $CaCl_2$, coagulation times were recorded. Points represent the mean ± SD of triplicate determinations.

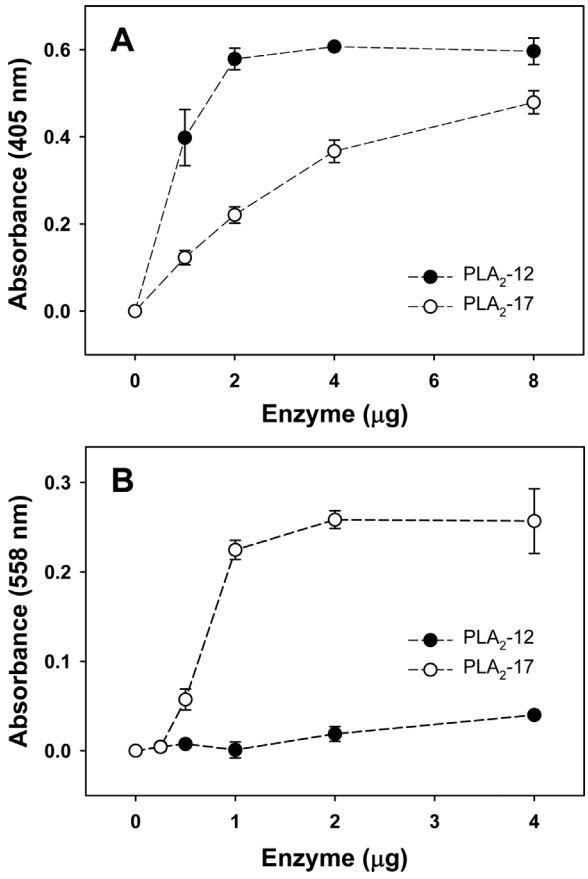


**Fig. 4.** Comparison of the phospholipase $A_2$ activity of $PLA_2$-12 or $PLA_2$-17 upon monodisperse and micellar substrates. **(A)** activity on 4-nitro-3-octanoyloxy-benzoic acid (NOBA), a synthetic monodisperse substrate. **(B)** activity on phosphatidylcholine micelles. Points represent mean ± SD of triplicate assays.

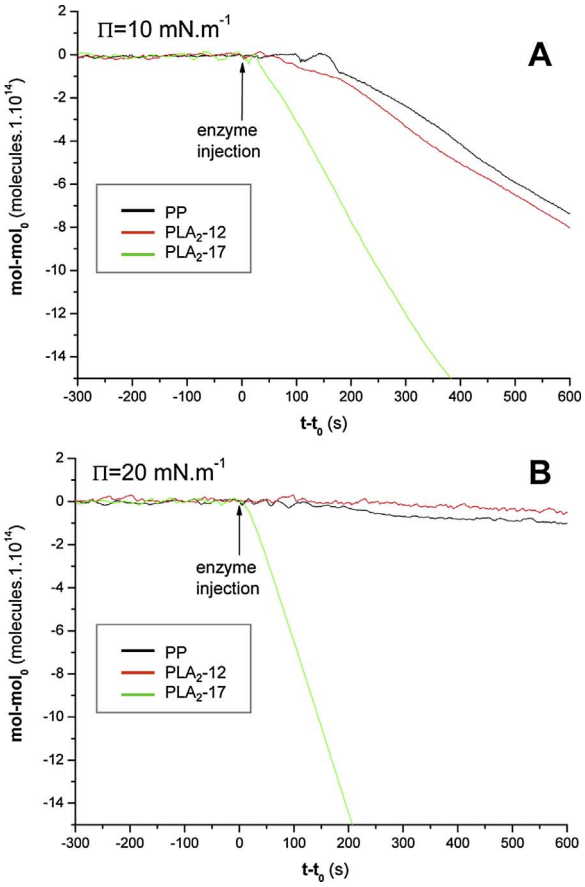


**Fig. 5.** Time course of the hydrolysis of DPLC monolayers catalyzed by $PLA_2$-12 and $PLA_2$-17 at constant lateral pressure (Π), expressed as molecules remaining at the surface of the trough minus molecules at the moment of injection ($mol_0$). The enzyme injection moment ($t_0$) is indicated by arrows. Pig pancreatic $sPLA_2$ (PP), a non-toxic group I enzyme, is included for comparison. Calculated hydrolytic rates are presented in Table 2. The linear portion after injection was fitted and the slope was used in calculation of the lipolytic ratio ($LR_{20/10}$) values for each $PLA_2$, presented in Table 3. For experimental conditions see text. Lateral pressure was maintained at 10 mN m$^{-1}$ in **(A)** or 20 mN m$^{-1}$ in **(B)**.

studied in three types of assays, all of them revealing striking differences. Using the monodisperse NOBA substrate, $PLA_2$-12 was significantly more active than $PLA_2$-17 (Fig. 4A), but results were the opposite when activity was assayed on phosphatidylcholine micelles, where $PLA_2$-17 was strongly hydrolytic in comparison to $PLA_2$-12, which was barely active (Fig. 4B).

Major differences between these two enzymes were also revealed when their ability to hydrolyze artificial phosphatidylcholine monolayers under varying lateral pressures was investigated. At a pressure of 10 mN m$^{-1}$, $PLA_2$-17 presented a much higher hydrolysis rate than $PLA_2$-12, whose catalytic rate was slower and very similar to that of the porcine pancreatic enzyme (Fig. 5A; Table 2). When the lateral pressure of the monolayer was increased to 20 mN m$^{-1}$, the difference between $PLA_2$-17 and $PLA_2$-12 became even more clear, since the latter enzyme, in similarity to the porcine pancreatic $PLA_2$, was virtually unable to hydrolyze the DPLC substrate. In marked contrast, under the same conditions $PLA_2$-17 continued to be highly active (Fig. 5B; and Table 2).

**Table 2**
Hydrolytic rate of phospholipase $A_2$ enzymes using lipid monolayers at different packing.

| $PLA_2$ enzyme | Lateral Pressure (mN m$^{-1}$) | Rate post-enzyme injection (molecule/s) $10^{14}$ |
|---|---|---|
| Pig Pancreatic $sPLA_2$ | 10 | $-1.67 \times 10^{-2}$ |
| Pig Pancreatic $sPLA_2$ | 20 | $-1.26 \times 10^{-3}$ |
| *M. fulvius* $PLA_2$-12 | 10 | $-1.62 \times 10^{-2}$ |
| *M. fulvius* $PLA_2$-12 | 20 | $-1.19 \times 10^{-3}$ |
| *M. fulvius* $PLA_2$-17 | 10 | $-4.23 \times 10^{-2}$ |
| *M. fulvius* $PLA_2$-17 | 20 | $-7.12 \times 10^{-2}$ |

### 3.4. Structural comparisons

$PLA_2$-12 and $PLA_2$-17 share a high degree of sequence conservation (79% identical and 86% similar residues; Fig. 6A). To explore possible structural differences that could be related to their contrasting functional characteristics, the three-dimensional structures of both proteins were modeled by homology using SWISSmodeler (Fig. 6B–D). The models generated for $PLA_2$-12 and $PLA_2$-17 suggest that both proteins adopt a highly similar fold, characteristic for secreted $PLA_2$s, with an rmsd of 0.7 Å (Fig. 6B). Superposition with the crystal structure of a $PLA_2$ from *Naja naja atra* in complex with a transition state analogue (PDBID 1POB) shows that both isoforms from *M. fulvius* have a conserved substrate binding site and catalytic center, and are thus expected to employ the canonical interfacial catalysis mechanism common to $PLA_2$s (Fig. 6C and D).

Despite their structural similarity, $PLA_2$-12 and $PLA_2$-17 show distinct surface properties. Interestingly, most of the variable positions map to the vicinity of the substrate binding pocket and interface recognition site (Figs. 6A and 7A). In this region, $PLA_2$-12 shows a prominent positively charged surface potential, whereas $PLA_2$-17 is much more acidic (Fig. 7B). Negative charge would not favor the interaction of $PLA_2$-17 with negatively-charged lipid membranes. Instead, $PLA_2$-17 carries several additional tryptophan residues – W18, W60, and W63 (L18, F60, and W63, respectively, in $PLA_2$-12) – at the membrane

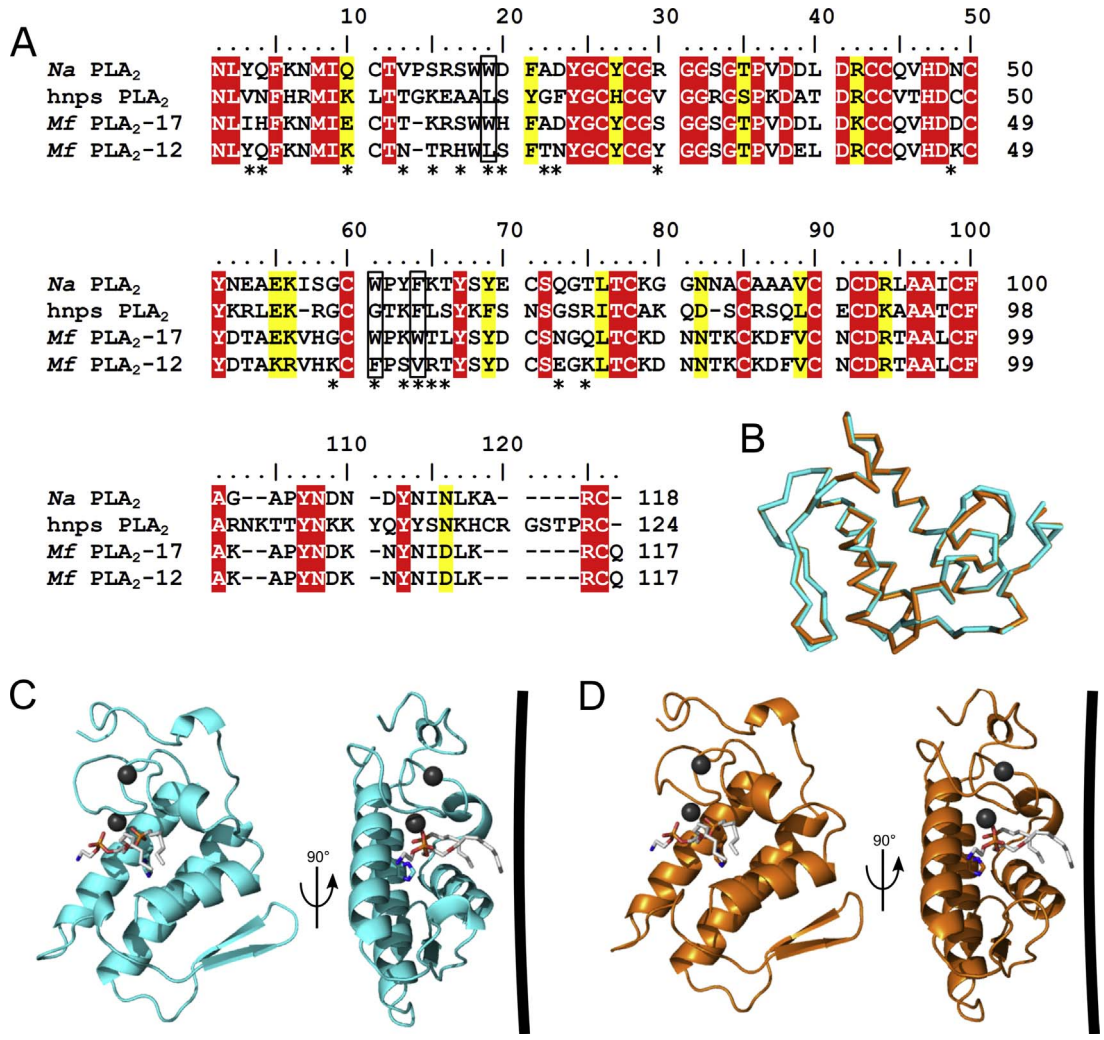


**Fig. 6.** Amino acid sequence alignment and homology three-dimensional structural models generated for $PLA_2$-12 and $PLA_2$-17 from *Micrurus fulvius* (*Mf*). **(A)** Sequence alignment of *Mf* $PLA_2$-12 and *Mf* $PLA_2$-17, *Naja atra* $PLA_2$ and human nonpancreatic secreted (hnps) $PLA_2$. Identical and similar residues are shaded red and yellow, respectively. Positions that vary between $PLA_2$-12 and $PLA_2$-17 are marked by asterisk, and three key positions are boxed. **(B)** Models generated for $PLA_2$-12 and $PLA_2$-17 by SWISSmodeler suggest that both proteins adopt a highly similar fold characteristic for phospholipases $A_2$, with an rmsd of 0.7 Å. **(C)** View of predicted membrane facing side of $PLA_2$-12 and a side view with the black line representing the membrane surface. The position of the catalytic His, two $Ca^{2+}$ ions and a transition state analogue are modelled by comparison with PDB ID:1pob. **(D)** as in **C**, but for $PLA_2$-17.

interface site that could promote membrane interaction by insertion into the lipid bilayer. Tryptophan is known to favor interfacial interactions with phospholipid bilayers by its tendency to insert (Yau et al., 1998; Beers et al., 2003; Nemec et al., 2006)

## 4. Discussion

Being nearly universally present in snake venoms, $PLA_2$s represent one of the most successful protein scaffolds recruited and diversified to display a variety of toxic effects, by evolving subtle differences on a remarkably conserved architecture (Nakashima et al., 1995; Kini and Chan, 1999). However, the structure-function relationships of toxic $PLA_2$s are only partially understood, and the precise determinants that endow these enzymes with particular bioactivities are mostly unknown. In this regard, venom $PLA_2$s have been considered 'a complex multifunctional protein puzzle' (Kini, 1997).

Viperid and elapid snakes often possess numerous genes encoding different $PLA_2$ isoforms expressed in the venom gland (Chen et al., 2004; Malhotra et al., 2015), ranging from acidic to highly basic variants. Furthermore, in many species variants exist that lack the ability to catalyze phospholipid hydrolysis but nevertheless display toxic activities, for example the subfamily of Lys49 $PLA_2$ homologues in viperids (dos Santos et al., 2009; Lomonte and Rangel, 2012), or the $PLA_2$-like component of a nociceptive complex found in some elapids (Bohlen et al., 2011).

The venom of the Eastern coral snake, *M. fulvius*, represents a clear case for the diversity of $PLA_2$ isoforms, with more than 50 different transcripts sequenced from its venom gland (Margres et al., 2013). A unique feature of this venom is its ability to induce severe intravascular hemolysis in some mammalian species, such as dogs and mice. A previous investigation demonstrated that distinct $PLA_2$s are responsible for the lysis of red blood cells occurring in experimental envenoming of mice (Arce-Bejarano et al., 2014). In the present study, we have purified and compared the functional profiles of $PLA_2$-17, a direct hemolytic enzyme from *M. fulvius* venom, and $PLA_2$-12, a co-existing enzyme lacking such effect.

Results showed that $PLA_2$-12 and $PLA_2$-17, two major venom components, differ not only in ability to cause intravascular hemolysis, but also in several other toxic properties. $PLA_2$-17 displayed hemolytic, lethal, myotoxic, and anticoagulant actions, whereas $PLA_2$-12 lacked all these effects, despite both being catalytically-active. This further exemplifies the wide functional diversity of $PLA_2$s in snake venoms, whereby different variants may range from highly toxic to seemingly harmless enzymes. It has been speculatively argued that $PLA_2$s

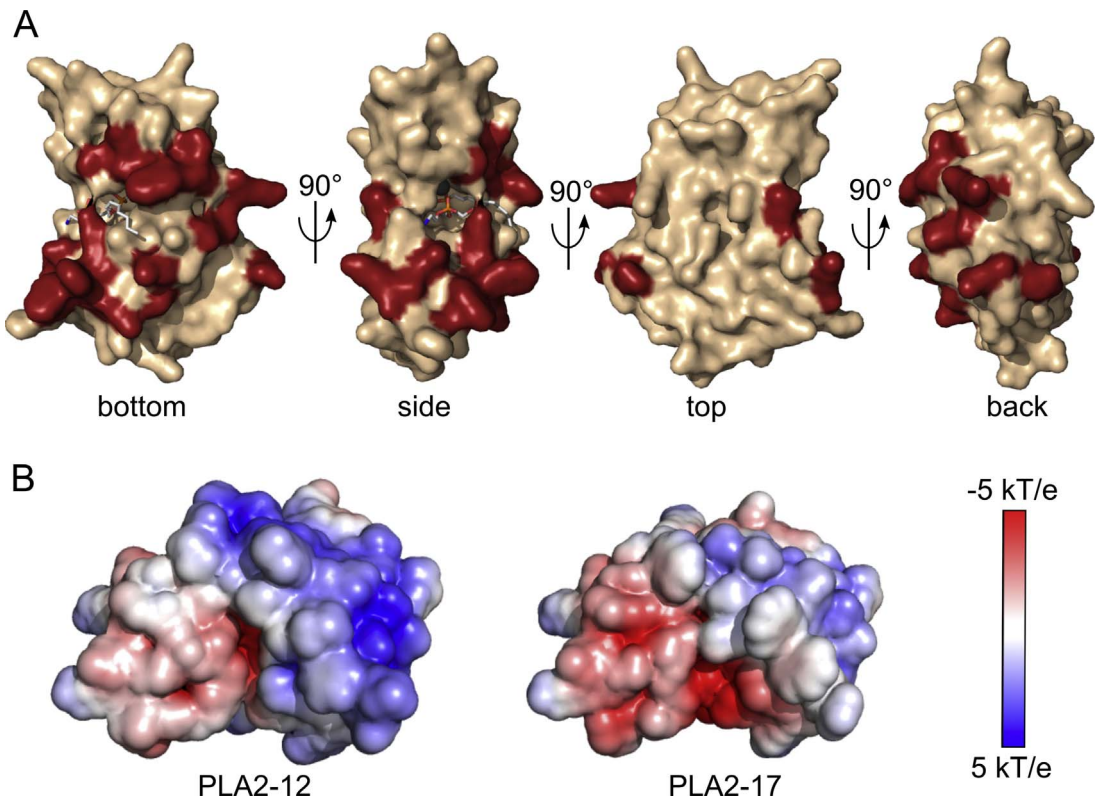


**Fig. 7.** Comparison of surface properties of $PLA_2$-12 and $PLA_2$-17 from *Micrurus fulvius*. **(A)** Variable positions shown in red are mapped on the surface of $PLA_2$-17, showing clustering of amino acid substitutions on the membrane interacting face (viewed as 'bottom'). **(B)** Surface potential map of $PLA_2$-12 and $PLA_2$-17 at the membrane interacting face. Compared to $PLA_2$-12, $PLA_2$-17 shows a more acidic charge distribution, which is expected to oppose phospholipid interaction, but exposes more aromatic side chains, which could promote membrane interaction.

apparently devoid of toxic effects could serve a digestive purpose, could have yet unknown actions on particular prey, or could represent recruited enzymes expressed in the venom gland that did not evolve towards toxicity (Fernández et al., 2010; Van der Laat et al., 2013). In addition, the possibility of synergistic actions with other components (Bustillo et al., 2015) could also give adaptive significance to the presence of such non-toxic $PLA_2$ enzymes in venoms, sometimes even in considerable amounts. In the present case, $PLA_2$-12 represents ~13% of the total venom proteins, as estimated by RP-HPLC, being nearly as abundant as the highly toxic $PLA_2$-17 (~23%).

Neither $PLA_2$-12 or $PLA_2$-17 showed bactericidal activity, contrary to the whole venom, which likely exerts this effect by means of other antimicrobial components such as L-amino acid oxidase (de Oliveira Junior et al., 2013). This finding may point out to a functional difference between group I (from elapids) and group II (from viperids) $PLA_2$s, since the latter often display bactericidal effects (Páramo et al., 1998; Samy et al., 2008), in similarity to group II $PLA_2$s of mammalian origin (Nevalainen et al., 2008). However, at least in the case of the elapid *Bungarus fasciatus*, a homodimeric group I $PLA_2$ demonstrated bactericidal effects (Xu et al., 2007), illustrating the wide diversity of actions among closely related enzyme isoforms in snake venoms.

The two enzymes here characterized showed prominent differences in their catalytic actions when assayed in three different settings. The non-toxic $PLA_2$-12 was much more active than $PLA_2$-17 in hydrolyzing NOBA, a monodisperse synthetic substrate, but the activity of $PLA_2$-17 was markedly higher when acting upon a micellar phosphatidylcholine substrate. This underscores the higher capacity of $PLA_2$-17 to hydrolyze aggregated phospholipids, which resemble more closely the lipid organization of membranes in cells. Experiments with the DLPC artificial monolayers were even more revealing, showing conspicuous differences in the ability of the two enzymes to exert hydrolysis at different lateral pressures. The behavior of $PLA_2$-12 in the monolayer assay was very similar to that of the non-toxic pancreatic $PLA_2$, reinforcing the proposal that this experimental setup could be relevant to predict differences in the toxicity of $PLA_2$s (Yunes Quartino et al., 2015). Moreover, when hydrolysis was tested at a lateral pressure of 20 mN $m^{-1}$ in the phospholipid monolayer, both $PLA_2$-12 and the pancreatic $PLA_2$ essentially halted their activity, whereas the toxic $PLA_2$-17 did not. These results can be interpreted as an indication of differences in the ability to penetrate the phospholipid monolayer (Verheij et al., 1980) for toxic and non-toxic $PLA_2$s. $PLA_2$-17, with a presumably stronger penetrating power, could withstand the higher pressure conditions that basically prevented a productive access to substrate of the weaker $PLA_2$-12 or the pancreatic enzyme. The lipolytic ratio ($LR_{(20/10)}$) values obtained for $PLA_2$-12 and $PLA_2$-17, respectively, are compared to those of other $PLA_2$s assayed identically in a previous study (Yunes Quartino et al., 2015), in Table 3. The toxic enzymes present higher $LR_{(20/10)}$ values than non-toxic counterparts. Taken together, our observations suggest that the differential toxicity of these $PLA_2$s is mainly due to their variable capacity to penetrate phospholipid membranes of different types of cells (erythrocytes, muscle fibers and possibly nerve terminals) and of aggregated plasma phospholipids, hence the different anticoagulant activity.

The different functional profiles of $PLA_2$-12 and $PLA_2$-17 called for a comparative examination of their primary structures, as well as their predicted three-dimensional folding, which could reveal interesting clues. The amino acid sequence of their N-terminal and central regions, which constitute the membrane interaction interface, presents more differences than their C-terminal regions, which are completely conserved after position 75 (Fig. 6A). These differences do not predict major shifts in the overall backbones, which are virtually superimposable (rmsd = 0.7 Å; Fig. 6B), but originate several interesting variations of the surface properties at the catalytic face. The interfacial binding surface of $PLA_2$s has been described to include aromatic and

**Table 3**
Comparison of Lipolytic ratio ($LR_{(20/10)}$) values for secreted phospholipase $A_2$ enzymes from different sources, on DLPC monolayers.[a]

| $PLA_2$ enzyme source | $LR_{(20/10)}$ |
|---|---|
| Pig pancreatic | 0.08 |
| *M. fulvius* $PLA_2$-12 | 0.07 |
| *M. fulvius* $PLA_2$-17 | 1.68 |
| *Bothrops diporus* $PLA_2$-I and II [b] | 0 |
| Bee (*Apis mellifera*) venom [b] | 1.1 |
| *Naja naja* [b] | 1.5 |
| *Bothrops diporus* $sPLA_2$-III [b] | 1.3 |
| *Bothrops asper* sPLA2-III [b] | 1.3 |
| *Naja. m. mossambica* [b] | 1.6 |

[a] All measurements were obtained in barostatic conditions (surface pressure kept constant during the time-course of hydrolysis at either 10 or 20 mN $m^{-1}$).
[b] Values from Yunes Quartino et al. (2015).

basic residues, which promote interaction. Changes in these residues can be expected to modulate interaction with membranes and thus catalytic efficiency on natural substrate surfaces. $PLA_2$-17 is less basic, but contains more bulky aromatic residues, which would have a decreasing and enhancing effect on membrane binding, respectively. However, $PLA_2$-17 is a more efficient enzyme on membrane surfaces, especially under high tension, probably due to a higher penetrating power, and also shows toxicity *in vivo*, while $PLA_2$-12 is a poor interfacial enzyme and not toxic. Interestingly, the comparison with a toxic (*Na* $PLA_2$) and a non-toxic $PLA_2$ (human nonpancreatic secretory; hnps $PLA_2$) reveals similar amino acid properties at the relevant positions (Fig. 6A): like $PLA_2$-17, *Na* $PLA_2$ has aromatic residues at the three variable positions in *Mf* $PLA_2$s, whereas hnps $PLA_2$ only has one phenylalanine, similar to $PLA_2$-12. We suggest that position 18 (W in $PLA_2$-17 and L in $PLA_2$-12) likely represents a key residue determining interfacial activity of *Mf* $PLA_2$s. Thus, the comparative analysis of the closely related, but functionally distinct $PLA_2$s from *M. fulvius* suggests that the ability of these enzymes to penetrate the substrate interface, facilitated by aromatic/hydrophobic residues at key positions for interaction, could be a major determinant of toxicity, perhaps more important than protein surface charge.

## Conflict of interest

The authors declare that there is no conflicts of interest.

## Acknowledgements

This work was funded by the International Centre for Genetic Engineering and Biotechnology (ICGEB; grant CRP/13/006) and Vicerrectoría de Investigación, Universidad de Costa Rica (VI-741-B4-100). The funding sources had no involvement in the study design, collection, analysis and interpretation of data, writing of the report and decision to submit the article for publication.

## Appendix A. Supplementary data

Supplementary data associated with this article can be found, in the online version, at https://doi.org/10.1016/j.toxlet.2017.11.037.

## References

Arce-Bejarano, R., Lomonte, B., Gutiérrez, J.M., 2014. Intravascular hemolysis induced by the venom of the eastern coral snake, *Micrurus fulvius*, in a mouse model: identification of directly hemolytic phospholipases $A_2$. Toxicon 90, 26–35.
Arnold, K., Bordoli, L., Kopp, J., Schwede, T., 2006. The SWISS-MODEL workspace: a web-based environment for protein structure homology modelling. Bioinformatics 22, 195–201.
Baker, N.A., Sept, D., Joseph, S., Holst, M.J., McCammon, J.A., 2001. Electrostatics of nanosystems: application to microtubules and the ribosome. Proc. Natl. Acad. Sci. U. S. A. 98, 10037–10041.
Beers, S.A., Buckland, A.G., Giles, N., Gelb, M.H., Wilton, D.C., 2003. Effect of tryptophan insertions on the properties of the human group IIA phospholipase $A_2$: mutagenesis produces an enzyme with characteristics similar to those of the human group V phospholipase $A_2$. Biochemistry 42, 7326–7338.
Bohlen, C.J., Chesler, A.T., Sharif-Naeini, R., Medzihradszky, K.F., Zhou, S., King, D., Sanchez, E.E., Burlingame, A.L., Basbaum, A.I., Julius, D., 2011. A heteromeric Texas coral snake toxin targets acid-sensing ion channels to produce pain. Nature 479, 410–414.
Bustillo, S., García-Denegri, M.E., Gay, C., Van de Velde, A.C., Acosta, O., Angulo, Y., Lomonte, B., Gutiérrez, J.M., Leiva, L., 2015. Phospholipase $A_2$ enhances the endothelial cell detachment effect of a snake venom metalloproteinase in the absence of catalysis. Chem. Biol. Interact. 240, 30–36.
Chen, Y.H., Wang, Y.M., Hseu, M.J., Tsai, I.H., 2004. Molecular evolution and structure-function relationships of crotoxin-like and asparagine-6-containing phospholipases $A_2$ in pit viper venoms. Biochem. J. 381, 25–34.
Condrea, E., Fletcher, J.E., Rapuano, B.E., Yang, C.C., Rosenberg, P., 1981. Dissociation of enzymatic activity from lethality and pharmacological properties by carbamylation of lysines in *Naja nigricollis* and *Naja naja atra* snake venom phospholipases $A_2$. Toxicon 19, 705–720.
DeLano, W.L., 2003. The PyMOL Molecular Graphics System. DeLano Scientific, San Carlos, California, USA.
Fernández, J., Gutiérrez, J.M., Angulo, Y., Sanz, L., Juárez, P., Calvete, J.J., Lomonte, B., 2010. Isolation of an acidic phospholipase $A_2$ from the venom of the snake *Bothrops asper* of Costa Rica: biochemical and toxicological characterization. Biochimie 92, 273–283.
Fernández, J., Vargas, N., Pla, D., Sasa, M., Rey-Suárez, P., Sanz, L., Gutiérrez, J.M., Calvete, J.J., Lomonte, B., 2015. Snake venomics of *Micrurus alleni* and *Micrurus mosquitensis* from the Caribbean region of Costa Rica reveals two divergent compositional patterns in new World elapids. Toxicon 107, 217–233.
Gao, R., Kini, R.M., Gopalakrishnakone, P., 1999. Purification, properties, and amino acid sequence of a hemoglobinuria-inducing phospholipase $A_2$ MiPLA-1, from *Micropechis ikaheka* venom. Arch. Biochem. Biophys. 369, 181–192.
Gutiérrez, J.M., Lomonte, B., 2013. Phospholipases $A_2$: unveiling the secrets of a functionally versatile group of snake venom toxins. Toxicon 62, 27–39.
Gutiérrez, J.M., Lomonte, B., Cerdas, L., 1986. Isolation and partial characterization of a myotoxin from the venom of the snake *Bothrops nummifer*. Toxicon 24, 885–894.
Kini, R.M., Chan, Y.M., 1999. Accelerated evolution and molecular surface of venom phospholipase $A_2$ enzymes. J. Mol. Evol. 48, 125–132.
Kini, R.M., 1997. Phospholipase $A_2$ – a complex multifunctional protein puzzle. In: Kini, R.M. (Ed.), Venom Phospholipase $A_2$ Enzymes: Structure, Function and Mechanism. John WileyChichester, UK, pp. p.1.
Kini, R.M., 2003. Excitement ahead: structure, function and mechanism of snake venom phospholipase $A_2$ enzymes. Toxicon 42, 827–840.
Križaj, I., 2014. Roles of secreted phospholipases $A_2$ in the mammalian immune system. Protein Pept. Lett. 21, 1201–1208.
Laemmli, U.K., 1970. Cleavage of structural proteins during the assembly of the head of bacteriophage T4. Nature 227, 680–685.
Lomonte, B., Rangel, J., 2012. Snake venom Lys49 myotoxins: from phospholipases $A_2$ to non-enzymatic membrane disruptors. Toxicon 60, 520–530.
Lomonte, B., Rey-Suárez, P., Fernández, J., Sasa, M., Pla, D., Vargas, N., Bénard-Valle, M., Sanz, L., Corrêa-Netto, C., Núñez, V., Alape-Girón, A., Alagón, A., Gutiérrez, J.M., Calvete, J.J., 2016. Venoms of *Micrurus* coral snakes: evolutionary trends in compositional patterns emerging from proteomic analyses. Toxicon 122, 7–25.
Malhotra, A., Creer, S., Harris, J.B., Thorpe, R.S., 2015. The importance of being genomic: non-coding and coding sequences suggest different models of toxin multi-gene family evolution. Toxicon 107, 344–358.
Margres, M.J., Aronow, K., Loyacano, J., Rokyta, D.R., 2013. The venom gland transcriptome of the eastern coral snake (*Micrurus fulvius*) reveals high venom complexity in the intragenomic evolution of venoms. BMC Genomics 14, 531.
Marks, S.L., Mannella, C., Schaer, M., 1990. Coral snake envenomation in the dog: report of four cases and review of the literature. J. Am. Anim. Hosp. Assoc. 26, 629–634.
Montecucco, C., Gutiérrez, J.M., Lomonte, B., 2008. Cellular pathology induced by snake venom phospholipase $A_2$ myotoxins and neurotoxins: common aspects of their mechanisms of action. Cell. Mol. Life Sci. 65, 2897–2912.
Mora-Obando, D., Díaz, C., Angulo, Y., Gutiérrez, J.M., Lomonte, B., 2014. Role of enzymatic activity in muscle damage and cytotoxicity induced by *Bothrops asper* Asp49 phospholipase $A_2$ myotoxins: are there additional effector mechanisms involved? PeerJ 2, e569.
Nakashima, K., Nobuhisa, I., Desimaru, M., Nakai, M., Ogawa, T., Shimohigashi, Y., Fukumaki, Y., Hattori, M., Sakaki, Y., Hattori, S., Ohno, M., 1995. Accelerated evolution in the protein-coding regions is universal in crotalinae snake venom gland phospholipase $A_2$ isoenzyme genes. Proc. Natl. Acad. Sci. U. S. A. 92, 5605–5609.
Nemec, K.N., Pande, A.H., Qin, S., Bieber Urbauer, R.J., Tan, S., Moe, D., Tatulian, S.A., 2006. Structural and functional effects of tryptophans inserted into the membrane-binding and substrate-binding sites of human group IIA phospholipase $A_2$. Biochemistry 45, 12448–12460.
Nevalainen, T.J., Graham, G.G., Scott, K.F., 2008. Antibacterial actions of secreted phospholipases $A_2$. Rev. Biochim. Biophys. Acta 1781, 1–9.
Páramo, L., Lomonte, B., Pizarro-Cerdá, J., Bengoechea, J.A., Gorvel, J.P., Moreno, E., 1998. Bactericidal activity of Lys49 and Asp49 myotoxic phospholipases $A_2$ from *Bothrops asper* snake venom: synthetic Lys49 myotoxin II-(115-129)-peptide identifies its bactericidal region. Eur. J. Biochem. 253, 452–461.
Pérez, M.L., Fox, K., Schaer, M., 2012. A retrospective evaluation of coral snake envenomation in dogs and cats (20 cases) (1996–2011). J. Vet. Med. Crit. Care 22, 682–689.

Peterson, M.E., 2006. Snake bite: coral snakes. Clin. Tech. Small Anim. Pract. 21, 183–186.
Rey-Suárez, P., Núñez, V., Fernández, J., Lomonte, B., 2016. Integrative characterization of the venom of the coral snake *Micrurus dumerilii* (Elapidae) from Colombia: proteome, toxicity, and cross-neutralization by antivenom. J. Proteomics 136, 262–273.
Samy, R., Gopalakrishnakone, P., Ho, B., Chow, V.T., 2008. Purification, characterization and bactericidal activities of basic phospholipase $A_2$ from the venom of *Agkistrodon halys* (Chinese pallas). Biochimie 90, 1372–1388.
Van der Laat, M., Fernández, J., Durban, J., Villalobos, E., Camacho, E., Calvete, J.J., Lomonte, B., 2013. Amino acid sequence and biological characterization of BlatPLA$_2$, a non-toxic acidic phospholipase $A_2$ from the venom of the arboreal snake *Bothriechis lateralis* from Costa Rica. Toxicon 73, 71–80.
Vargas, L.J., Londoño, M., Quintana, J.C., Rua, C., Segura, C., Lomonte, B., Núñez, V., 2012. An acidic phospholipase $A_2$ with antibacterial activity from Porthidium nasutum snake venom. Comp. Biochem. Physiol. 161 (B), 341–347.
Verheij, H.M., Boffa, M.C., Rothen, C., Bryckaert, M.C., Verger, R., de Haas, G.H., 1980. Correlation of enzymatic activity and anticoagulant properties of phospholipase $A_2$. Eur. J. Biochem. 112, 25–32.
White, S.P., Scott, D.L., Otwinowski, Z., Gelb, M.H., Sigler, P.B., 1990. Crystal structure of cobra-venom phospholipase $A_2$ in a complex with a transition-state analogue. Science 250, 1560–1563.
Xu, C., Ma, D., Yu, H., Li, Z., Liang, J., Lin, G., Zhang, Y., Lai, R., 2007. A bactericidal homodimeric phospholipase $A_2$ from *Bungarus fasciatus* venom. Peptides 28, 969–973.
Yau, W.M., Wimley, W.C., Gawrisch, K., White, S.H., 1998. The preference of tryptophan for membrane interfaces. Biochemistry 37, 14713–14718.
de Oliveira Junior, N.G., Silva Cardoso, M.H., Franco, O.L., 2013. Snake venoms: attractive antimicrobial proteinaceous compounds for therapeutic purposes. Cell. Mol. Life Sci. 70, 4645–4658.
dos Santos, J.I., Fernandes, C.A., Magro, A.J., Fontes, M.R., 2009. The intriguing phospholipases $A_2$ homologues: relevant structural features on myotoxicity and catalytic inactivity. Protein Pept. Lett. 16, 887–893.
Yunes Quartino, P.J., Portela, M., Lima, A., Durán, R., Lomonte, B., Fidelio, G.D., 2015. A constant area monolayer method to assess optimal lipid packing for lipolysis tested with several secreted phospholipases $A_2$. Biochim. Biophys. Acta Biomembr. 1848, 2216–2224.

# Intravascular hemolysis induced by phospholipases $A_2$ from the venom of the Eastern coral snake, *Micrurus fulvius*: functional profiles of hemolytic and non-hemolytic isoforms

María Laura Fernández[1], Pablo Yunes Quartino[2], Ruth Arce-Bejarano[1], Julián Fernández[1], Luis F. Camacho[1], José María Gutiérrez[1], Daniel Kuemmel[3], Gerardo Fidelio[2], Bruno Lomonte[1*]

[1] Instituto Clodomiro Picado, Facultad de Microbiología, Universidad de Costa Rica, San José 11501, Costa Rica; [2] Centro de Investigaciones en Química Biológica de Córdoba (CIQUIBIC), Departamento de Química Biológica, Facultad de Ciencias Químicas, Universidad Nacional de Córdoba, Argentina; [3] Biology and Chemistry Department, University of Osnabrueck, Osnabrueck, Germany

## Supplementary Figures

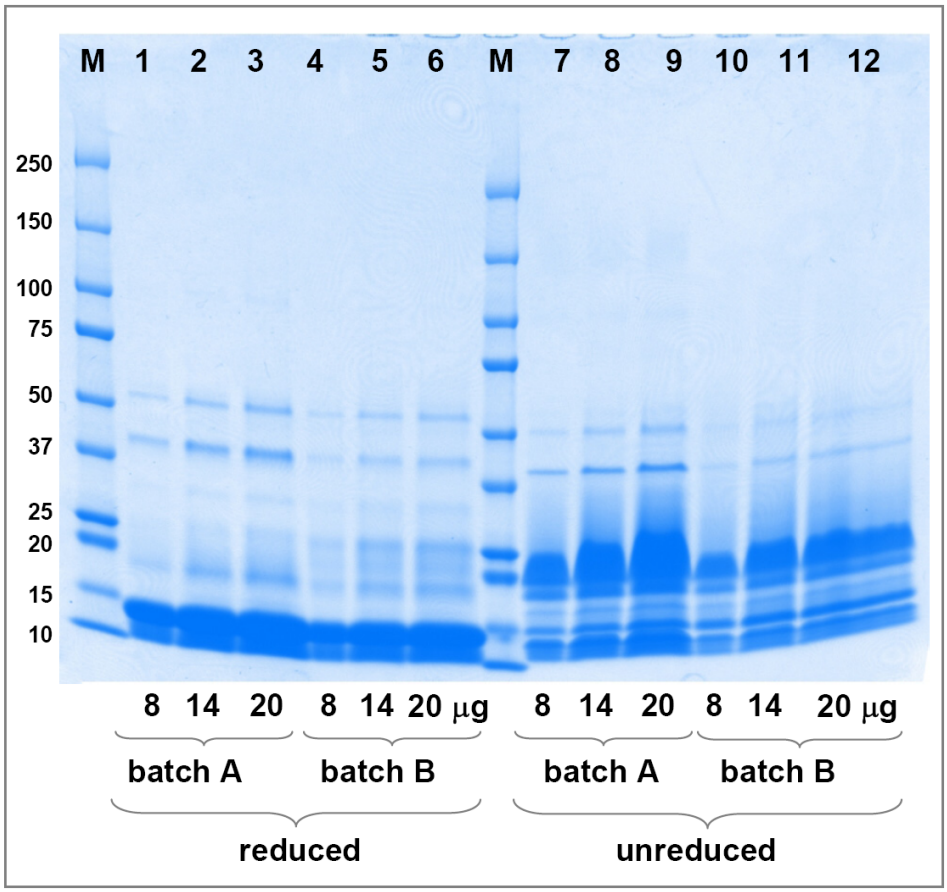


**Figure S1:** SDS-polyacrylamide gel electrophoresis of *Micrurus fulvius* venom under reducing (lanes 1-6) or non-reducing conditions (lanes 7-12). Two batches of venom used in this study were compared, A (Sigma) and B (NIH), as described in Methods, loading 8, 14, or 20 µg per lane. Proteins were stained with Coomassie blue G-250. M: molecular weight markers (M) are labeled in kDa at the left. The venom patterns of both batches are qualitatively conserved.

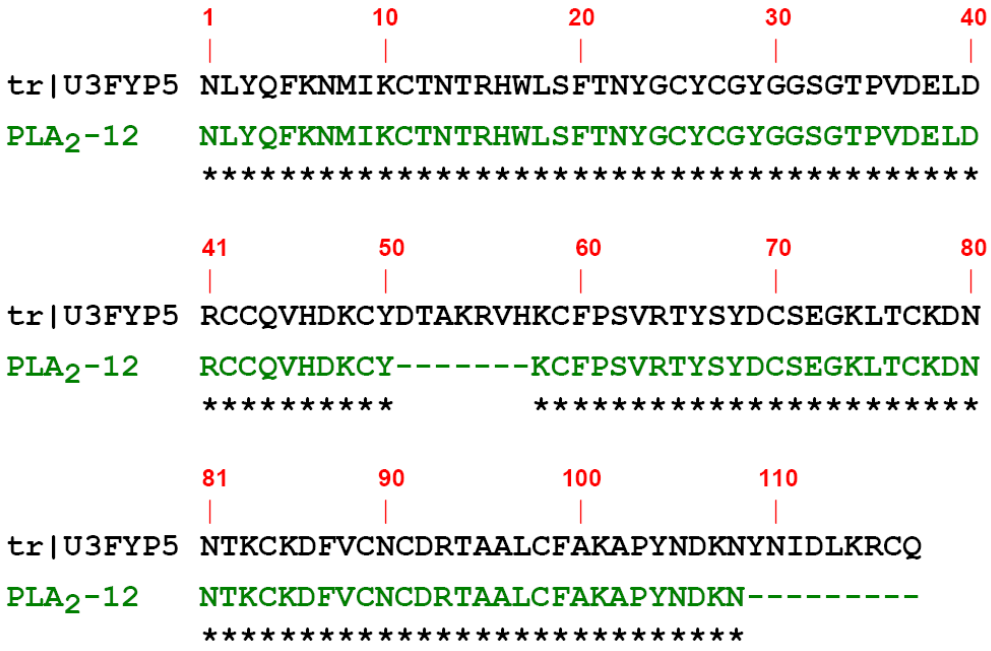


**Figure S2:** Identification of $PLA_2$-12, isolated from the venom of *Micrurus fulvius*, as U3FYP5 (=$PLA_2$-24) in the venom gland transcriptome reported by Margres et al. (2013). Partial amino acid sequence of the protein was obtained by digestion with trypsin or chymotrypsin, followed by MALDI-TOF/TOF analysis of the resulting peptides, as described in Methods. Amino acid positions not identified in $PLA_2$-12 are indicated by dashes. Alignment of the partial sequence obtained for $PLA_2$-12 matched a single venom gland transcript from *M. fulvius*, access code U3FYP5. Asterisks denote identical amino acids in the alignment.